

Elemental bio-imaging of calcium phosphate crystal deposits in knee samples from arthritic patients

Christine Austin,^a Dominc Hare,^a Andrew L Rozelle,^b William H Robinson,^b Rudolf Grimm,^c and Philip Doble^a

Received (in XXX, XXX) Xth XXXXXXXXXX 200X, Accepted Xth XXXXXXXXXX 200X

First published on the web Xth XXXXXXXXXX 200X

DOI: 10.1039/b000000x

Laser ablation inductively coupled plasma mass spectrometry (LA ICP-MS) was employed to image deposits of calcium phosphate based crystals in knee cartilage and synovial fluid from arthritic patients. A reaction / collision cell that contained hydrogen minimised plasma interferences on calcium and also improved the image quality without significant sensitivity reduction. Areas of high calcium and phosphorus intensities consistent with crystal deposits were observed for both the cartilage and synovial fluid samples. These areas were also characterised by high magnesium and strontium intensities. Distribution patterns of other elements such as copper and sulfur did not correlate with the crystal deposits. Filtered and non-filtered solutions of calcium phosphate crystals grown in synthetic synovial fluid were also imaged as further evidence of crystals deposits. The crystal deposits were detected in the unfiltered solution, and absent from the filtered solutions.

Introduction

The importance of calcium pyrophosphate dihydrate (CPPD) and basic calcium phosphates (BCP) in rheumatology was first discovered in the early 1960's¹. Since then, the concurrence of BCP (hydroxyapatite, octacalcium phosphate, tricalcium phosphate) and CPPD crystals and degenerative joint disease has been well established. Though there is ample data available to support the role of BCP crystals in cartilage degeneration, it is still unclear whether other calcium-containing crystals play a direct driving role in disease conception and progression, or are merely markers of joint damage²⁻⁴.

The identification of specific crystal types in synovial fluid is currently the most popular method of diagnosing all common forms of crystal-associated arthritis³. In general, crystal arthritides cannot be distinguished from other causes of arthritis based on history or physical examination⁵. Despite the multitude of techniques that have been applied to BCP and CPPD crystal detection, clinical diagnosis almost exclusively relies on light microscopy (LM). However, LM lacks the resolution required to image small crystals (<1µm), is non-specific (though CPPD crystals can generally be distinguished under polarised LM) and accuracy is operator dependent^{3, 5-7}. Sensitivity can be improved by staining the sample with calcium specific dyes particularly for BCP crystals which are often too small to be seen by LM. However these are often subject to false positives.

Other techniques for the determination of BCP crystals include scanning electron microscopy (SEM) and transmission electron microscopy (TEM). These methods are expensive, complex and not widely available for routine analysis in a clinical setting. Techniques recently applied to crystal detection and identification include atomic force microscopy

(AFM), Fourier-transform infrared spectroscopy (FTIR) and Raman spectroscopy. AFM and Raman show great potential for this application. Additionally, FTIR and Raman spectrometers may be made compact, making the technology capable of point-of-care operation³. A comprehensive review of the analytical tools available for the detection and identification of calcium phosphate crystals was recently published by Yavorskyy, et al³. The review made it evident that a simple, inexpensive technique which is capable of detecting and identifying calcium phosphate-based crystals accurately and with a high sensitivity would be invaluable in the diagnosis of crystal associated arthritides.

Laser ablation inductively coupled plasma mass spectrometry (LA ICP-MS) is increasingly applied to the study of metals in biological samples^{8, 9}. LA ICP-MS offers direct multielemental analysis of solids and liquids with trace and ultra trace detection capabilities, and a linear dynamic range of seven or more orders of magnitude. Though its application to imaging of soft tissues is emerging, it is considered a mature technique for the analysis of geological and metallurgical samples¹⁰. In LA ICP-MS systems, a focussed laser beam is used to mobilise sample material as droplets or vapour from the sample surface⁹. The material is then transported to the plasma (usually by argon carrier gas) where the material is ionised and carried through to the mass spectrometer which selectively detects ions at a given mass-to-charge ratio.

LA ICP-MS may be utilised to construct maps that provide elemental spatial information at trace and bulk levels of biological samples such as small tumours in rat brains¹¹, β-amyloid plaques in mouse models of Alzheimer's disease¹², and the distribution of platinum in mouse kidneys treated with *cis*-platin¹³. The environmental sciences have also utilised the potential of this technique to analyse the environmental changes or pollutant accumulation evident from the changing

metal concentrations in increment growth layers of many types of organisms such as scales, shells, otoliths and tree xylem¹⁴.

Recently, Chaudhri et al.,¹⁵ determined the elemental distribution of bladder and kidney stones by LA ICP-MS. LA ICP-MS has also been employed to study element time profiles in teeth¹⁶ and bones¹⁷, and to determine strontium ratios in calcium phosphates¹⁸. Quantitative analysis of heavy metals in bone employing reference standards and spiking hydroxapatite standards has also been reported^{19, 20 17}. However, LA-ICP-MS has not been used to image crystal deposits in biological samples. Element concentrations in synovial fluids from osteoarthritic patients have been determined by ICP-MS²¹.

This study demonstrates the potential of LA ICP-MS for crystal detection in biological samples. Cartilage sections were obtained from knee or hip arthroplasty and were imaged by LA ICP-MS for the presence of crystal-associated elements. Additionally, eight synovial fluid samples, six from patients diagnosed with osteoarthritis (OA) and two from patients diagnosed with rheumatoid arthritis (RA), were

analysed by the same method. Results from each sample type are presented here. We propose that this method of analysis be termed "Elemental Bioimaging".

Experimental

Instrumental and measurement procedure

A quadrupole 7500ce ICP-MS (Agilent Technologies) with octopole collision/reaction cell and cs lenses installed was coupled to a New Wave UP213 laser ablation unit for the generation of elemental images of biological samples from arthritic patients.

Laser ablation of biological samples was performed using a frequency quintupled Nd:YAG laser with ablated material transported to the ICP-MS via a stream of argon carrier gas. The ICP-MS was operated in reaction gas mode to reduce the interferences on calcium and strontium isotopes. The optimised experimental parameters for LA ICP-MS analysis were recorded in Table 1. Cartilage samples (generally less than 10×10mm) were imaged in approximately 20hrs, whilst synovial fluid took approximately 2.5hrs to image.

Table XX Caption

Agilent 7500ce ICP-MS		New Wave UP213 Laser Ablation	
Rf Power	1370W	Wavelength	213nm
Cooling gas flow rate	15 l min ⁻¹	Repetition frequency	20Hz
Carrier gas flow rate	1.25 l min ⁻¹	Laser energy density	0.2J cm ⁻² (at 30%)
Hydrogen flow rate	2.5ml min ⁻¹	Cartilage Samples	
Sample Depth	5.0mm	Spot size	55 μm
QP Bias	-16V	Scan rate	30 μm s ⁻¹
OctP Bias	-20V	Synovial Fluid	
Scan mode	Peak hopping	Spot size	100 μm
Dwell time	0.1s, 0.2s for P	Scan rate	40 μm s ⁻¹
		Synthetic Synovial Fluid	
		Spot size	55 μm
		Scan rate	50 μm s ⁻¹

Imaging was performed using the software package ENVI v4.2 (Research Systems Inc., Boulder, CO, USA). The samples were systematically scanned across the entire area of the sample. For cartilage samples, the distance between adjacent scan lines was 29μm, which ensured complete ablation of the tissue sample. For the synovial spots, the line scans were placed 50 μm apart. The data files generated by ChemStation (Agilent Technologies) were then collected and imported into ENVI. As no quantification data was collected, images only show relative signal intensities.

Sample Preparation

All experiments were performed in compliance with the relevant laws and institutional guidelines of the University of Technology Sydney and Stanford University. The study was approved by the ethics committees of the University of Technology Sydney and Stanford University. Human samples were collected at Stanford University after informed consent and under Institutional Review Board (IRB)-approved protocols. Cartilage sections were obtained after either knee or hip arthroplasty. Sections were cut to 14μm thick dried.

Synovial fluid was aspirated from inflamed knee joints, centrifuged at 2000rpm and the supernatant collected and frozen, within 4 hours of collection, for storage. Synovial fluid was dropped (12μl) onto quartz cover slips and dried for analysis by LA ICP-MS.

Synthetic synovial fluid was prepared from human serum (Sigma, Germany) by mixing equal volumes (30%) of laboratory grade (Ajax, Sydney) 10mM calcium chloride, 50mM tetrasodium pyrophosphate and 7mM magnesium sulphate according to a method reported by Cheng for crystal formation of CPPD in aqueous solutions^{22, 23}. Tris(hydroxymethyl)methylamine (Ajax, Sydney) was added to maintain the pH around physiological levels. The calcium, magnesium and pyrophosphate salts were chosen based on the assumption that their counter ions would not form precipitates in the synthetic synovial solution. The synthetic synovial fluid was then left in the oven at 37°C for 2 weeks to encourage crystal formation. A disposable 0.22μm syringe filter was used to remove any large particles from solution. Both filtered and non-filtered solutions were dropped (5μl) onto a clean quartz slide and air dried before analysis by LA ICP-MS.

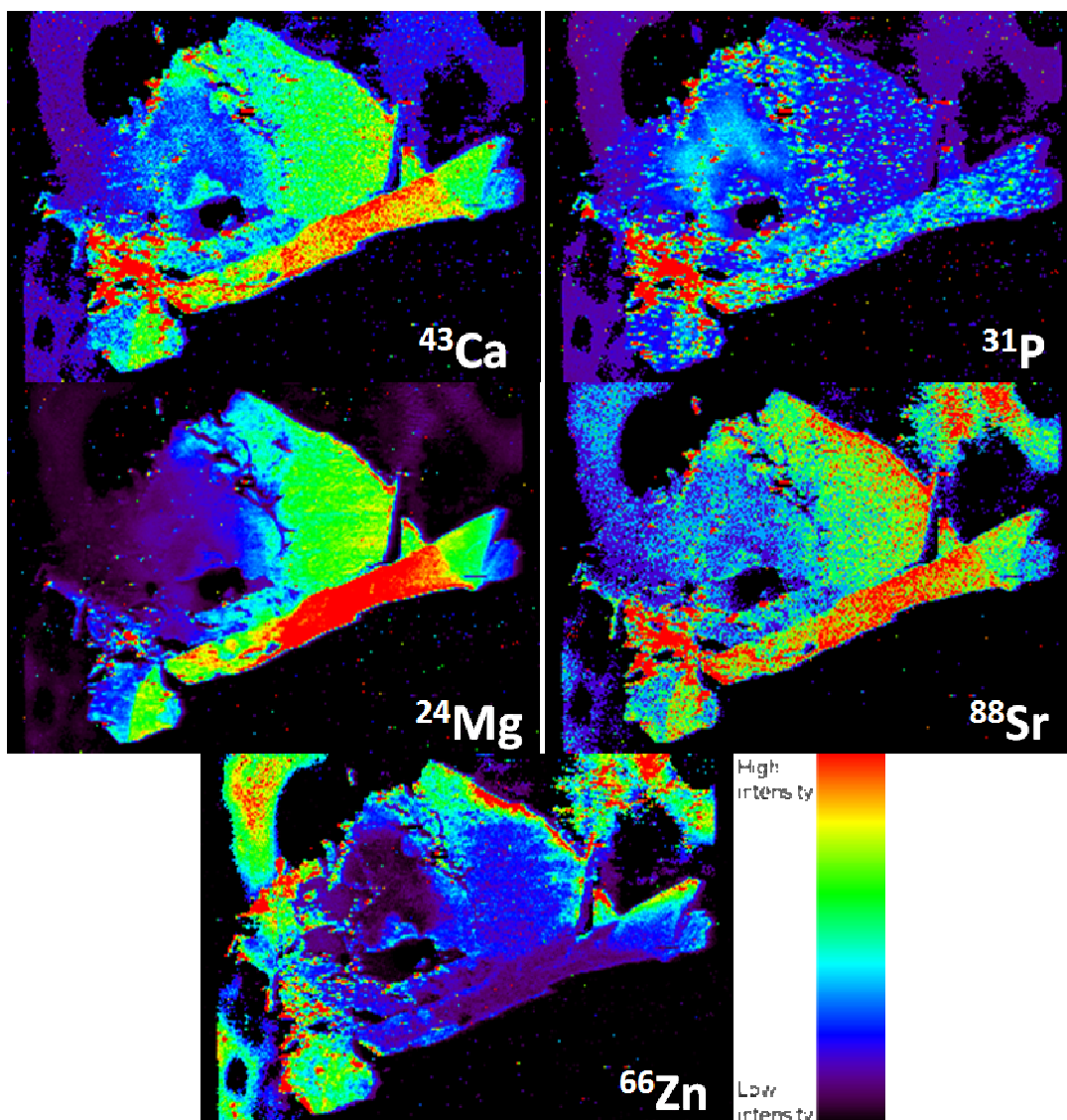


Fig. 1 Elemental distribution maps of calcium (^{43}Ca), phosphorus (^{31}P), magnesium (^{24}Mg), strontium (^{88}Sr) and zinc (^{66}Zn) in a knee cartilage section from a patient diagnosed with osteoarthritis

Results and Discussion

Imaging of Cartilage Samples

Cartilage examination for crystals can provide important information regarding the progression of the disease. For example, the density of crystals has been shown to correlate with the degree of mechanical stress exerted on the involved joint².

Initial experiments attempted to generate images with the reaction cell operating only as an ion guide. The calcium image signal was poor in quality due to a high background. Investigations into methods of background attenuation for calcium lead to experimentation with the octopole collision / reaction cell with hydrogen and helium, as well as utilising the cool plasma technique²⁴⁻²⁷. Experiments were performed using an in-house prepared plastic standard which contained all the elements of interest.

Use of a cool plasma and helium collision gas decreased the

background signal for calcium. However, sensitivity was significantly reduced for other elements. Hydrogen reaction gas significantly minimised the m/z 40 and m/z 44 background on calcium and interferences on strontium without significant loss of sensitivity. A hydrogen flow rate of 2.5ml/min gave the best compromise of attenuation of background and minimal matrix interference whilst maintaining signal sensitivity.

Elemental distribution maps of calcium, phosphorus, magnesium and strontium in a cartilage sample are presented in Figure 1. Element signals were normalised to ^{13}C as an internal standard to compensate for changes in mass ablated or signal drift^{28, 29}. Many of the tissue samples showed areas where it had folded or twisted over itself, i.e the tissue was thicker in those areas. The use of ^{13}C as an internal standard compensated for the difference in tissue thickness.

Figure 1 shows corresponding regions of relatively high calcium and phosphorus intensities in the cartilage section taken from a patient with osteoarthritis. These common areas

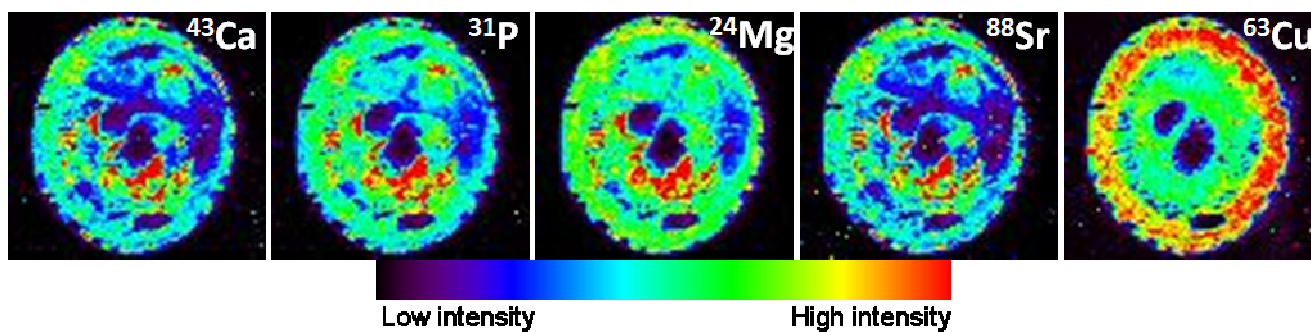


Fig. 2 Elemental distribution maps of calcium (^{43}Ca), phosphorus (^{31}P), magnesium (^{24}Mg), strontium (^{88}Sr) and copper (^{63}Cu) in a drop of osteoarthritic synovial fluid

5 may be representative of calcium phosphate-based crystal deposits. A high frequency of CPPD crystals in articular tissues removed from OA hips and knees has been reported in the literature³⁰. Other elements including copper, iron, and selenium did not follow the same trend in distribution.

10 The areas are significantly larger than the average crystal size (up to $20\mu\text{m}$)³. This may be due to aggregation of the crystals within the cartilage matrix. An alternative explanation was that the relatively larger laser spot size used for imaging of the smaller crystals swamped the ICP-MS signal. That is, 15 the crystals sizes were magnified by the use of a spot size larger than the average crystal size. This may be overcome by higher resolution imaging.

In addition, several regions of relatively high calcium and phosphate intensities correlated with relatively high 20 magnesium and strontium intensities. Magnesium whitlockite, a calcium orthophosphate crystal in which calcium is partly substituted with magnesium, has been reported in both osteoarthritic and normal articular cartilage and recent data suggest it may play a pathological role in arthritis³¹⁻³³. Our 25 results were consistent with the association of magnesium whitlockite and BCP crystals as areas of relatively high magnesium intensities consistently overlapped with areas of high calcium intensities.

Figure 1 also shows an area of relatively high strontium 30 intensity which corresponded to areas of high calcium, phosphorus and magnesium. To our knowledge the association of strontium with BCP crystals has not been reported before, however it has been detected in osteoarthritic synovial fluid²¹. Possible interferences of ^{88}Sr include double charged rare 35 earth elements, calcium dimers and argides, and calcium phosphates^{18, 34}. When tuning the ICP-MS on NIST 612, the formation of diatomic interferences was monitored and found to be minimal. The reaction cell was shown to further reduce this. The signal collected from m/z 88 was identified as 40 strontium as the $\text{Sr}^{88}/\text{Sr}^{86}$ isotope ratio agreed within the accepted range of natural abundances³⁵. Therefore, the strontium distribution maps appear to be genuine.

An interesting trend in the distribution of zinc was also observed in some samples. Areas of high calcium, phosphorus 45 and magnesium corresponded to regions of low zinc intensity.

This method also has the potential for ratio imaging. More objective and definitive detection of BCP crystals could be achieved by generating a 2D image of the Ca:P ratio, whereby areas with a ratio corresponding to that of BCP or CPPD

crystals are selectively coloured against the remaining tissue. This may allow CPPD crystals to be distinguished from BCP 55 crystals.

Imaging of Synovial Fluids

Synovial fluid is a more common sample type used by the 60 many existing analytical tools for crystal detection and research as it is more accessible to the clinician. Therefore, imaging by LA ICP-MS was also trialled on dried synovial drops.

Synovial fluid was collected from patients suffering from OA and rheumatoid arthritis. A small volume ($12\mu\text{l}$) was then 70 dropped onto a quartz coverslip and air dried. The laser experimental parameters ensured that the centre of the drop was completely ablated. The thicker outer-rim was not always ablated completely. No sample preparation was necessary, an advantage against other methods such as XRF, which requires the crystals to be first isolated³.

BCP crystals are uniquely associated with OA and have been reported to occur in up to 60% of patient synovial 80 samples^{3, 30}. CPPD crystals have been associated with 30% of OA synovial fluids³⁰. Images consistent with the presence of crystal deposits were observed for 1 of the OA samples and both of the RA samples. Though BCP crystals are uniquely associated with OA³, the presence of CPPD crystals in RA joint fluids is not uncommon as these crystals are often found in many arthritides³⁶.

Figure 2 shows the distribution of several elements in a drop of synovial fluid from an osteoarthritic joint. Similar 85 trends of common regions of relatively high calcium, phosphorus, magnesium and strontium were observed. An image of copper was included to illustrate the different distribution of elements not associated with calcium phosphate-based crystals.

85 Confirmation of Crystal Imaging Using Synthetic Synovial Fluid

Synovial fluid originates from plasma that is filtered by a capillary net and diffuses into the joint cavity, with the addition of locally synthesised hyaluronic acid, which is what 95 gives SF its characteristic viscosity⁷. Thus, synthetic synovial fluid samples were prepared using human serum to mimic the components of synovial fluid. After incubation of the solution, solid matter was observed.

The solution was filtered to remove the solid matter and

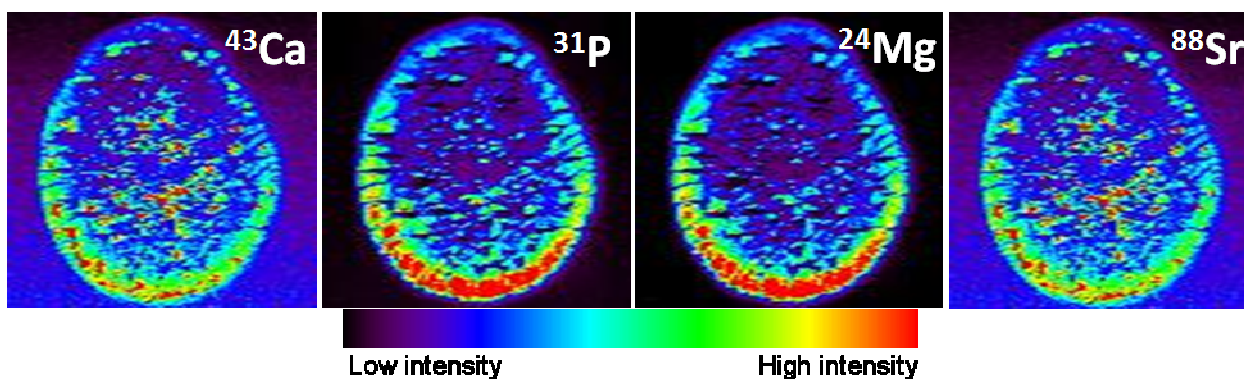


Fig. 3a Elemental distribution maps of calcium (^{43}Ca), phosphorus (^{31}P), magnesium (^{24}Mg) and strontium (^{88}Sr) in a drop of synthetic synovial fluid

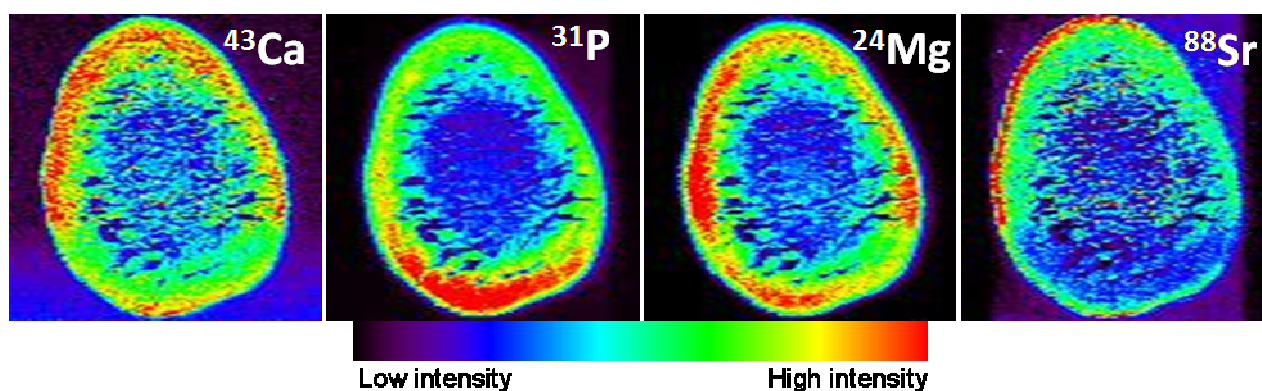


Fig. 3b Elemental distribution maps of calcium (^{43}Ca), phosphorus (^{31}P), magnesium (^{24}Mg) and strontium (^{88}Sr) in a drop of filtered synthetic synovial fluid

drops of both filtered and non-filtered solution were left to air dry on a clean slide. As the fluid was not as viscous as synovial fluid, the spot was not as thick and a faster scan rate could be applied whilst still ensuring complete ablation.

Images of the elemental distribution of calcium, phosphorus, magnesium and strontium are presented in Figure 3a. Again, results consistent with the presence of crystal deposits were observed in these images by common regions of relatively high intensities of crystal-associated elements.

In distinct contrast, the images produced from the ablation of the filtered solution do not show the small common regions that are consistent with crystal deposits (Figure 3b). These images instead show a more uniform distribution of the elements with increasing concentration radiating out from the centre of the spot, similar to that seen for non-crystal associated elements in the synovial fluid sample. Considering the common size of CPPD crystals, filtration at $0.22\mu\text{m}$ should remove any crystals or solid matter that formed in the solution.

The presence of CPPD or BCP crystals in the cartilage or synovial fluid samples was not confirmed by other methods currently used for this purpose. However, this preliminary study gives a good indication of the potential of LA ICP-MS to the detection of BCP and CPPD crystals in both cartilage and synovial fluid samples. Additionally, the calcium-to-phosphorus ratio may be used to identify the crystals present. Further studies are currently being pursued to confirm crystal

presence by SEM prior to laser ablation. This would validate the method in terms of false positives/negatives and sensitivity limits compared to other methods.

Additionally, quantification data may be obtained using standard serum solutions for spot calibration and matrix matched standardised tissue for cartilage samples.

Conclusions

This study has illustrated the potential of LA ICP-MS for the identification of crystal deposits in biological tissues and fluids through their localised elemental distributions. The distribution of BCP and CPPD crystal-associated elements, including calcium, phosphorus and magnesium, considered consistent with the presence of crystal deposits, was observed in osteoarthritic knee cartilage and synovial fluid samples by LA ICP-MS. Future studies will focus on quantification, validation of crystals by SEM and ratio imaging.

Notes and references

^a Elemental Bio-imaging Facility, Department of Chemistry, Materials and Forensic Science, University of Technology Sydney, Sydney, NSW 2007, Australia. Fax: +61 2 9514 1460; Tel: +61 2 9514 1792; E-mail: philip.doble@uts.edu.au

^b Division of Immunology and Rheumatology, Stanford University School of Medicine, 300 Pasteur Drive, Stanford, California 94305-5166, USA
^c Agilent Technologies, Inc.; Integrated Biology Solutions Unit, Santa Clara, California, USA

1. P. Dieppe and P. Calvert, *Crystals and joint disease*, Chapman and Hall, New York, 1983.
2. G. M. McCarthy, *Current Opinion in Rheumatology*, 1996, **8**, 255-258.
3. A. Yavorsky, A. Hernandez-Santana, G. McCarthy and G. McMahon, *Analyst (Cambridge, United Kingdom)*, 2008, **133**, 302-318.
4. C. W. Wu, R. Terkeltaub and K. C. Kalunian, *Current Rheumatology Reports*, 2005, **7**, 213-219.
5. A. K. Rosenthal and N. Mandel, *Current Rheumatology Reports*, 2001, **3**, 11-16.
6. P. Dieppe and A. Swan, *Annals of the Rheumatic Diseases*, 1999, **58**, 261-263.
7. E. Pascual and V. Jovani, *Best Practice & Research Clinical Rheumatology*, 2005, **19**, 371-386.
8. J. S. Becker, M. Zoriy, J. S. Becker, J. Dobrowolska and A. Matusch, *Journal of Analytical Atomic Spectrometry*, 2007, **22**, 736-744.
9. S. F. Durrant and N. I. Ward, *Journal of Analytical Atomic Spectrometry*, 2005, **20**, 821-829.
10. R. Lobinski, C. Moulin and R. Ortega, *Biochimie*, 2006, **88**, 1591-1604.
11. M. V. Zoriy, M. Dehnhardt, A. Matusch and J. S. Becker, *Spectrochimica Acta, Part B: Atomic Spectroscopy*, 2008, **63B**, 375-382.
12. R. W. Hutchinson, A. G. Cox, C. W. McLeod, P. S. Marshall, A. Harper, E. L. Dawson and D. R. Howlett, *Analytical Biochemistry*, 2005, **346**, 225-233.
13. M. Zoriy, A. Matusch, T. Spruss and J. S. Becker, *International Journal of Mass Spectrometry*, 2007, **260**, 102-106.
14. P. M. Outridge, G. Veinott and R. D. Evans, *Environmental Reviews (Ottawa)*, 1995, **3**, 160-170.
15. M. A. Chaudhri, J. Watling and F. A. Khan, *Journal of Radioanalytical and Nuclear Chemistry*, 2007, **271**, 713-720.
16. K. M. Lee, J. Appleton, M. Cooke, F. Keenan and K. Sawicka-Kapusta, *Analytica Chimica Acta*, 1999, **395**, 179-185.
17. C. Stadlbauer, C. Reiter, B. Patzak, G. Stinger and T. Prohaska, *Analytical and Bioanalytical Chemistry*, 2007, **388**, 593-602.
18. M. S. A. Horstwood, J. A. Evans and J. Montgomery, *Geochimica et Cosmochimica Acta*, 2008, **72**, 5659-5674.
19. D. J. Bellis, K. M. Hetter, J. Jones, D. Amarasiriwardena and P. J. Parsons, *Journal of Analytical Atomic Spectrometry*, 2006, **21**, 948-954.
20. T. Uryu, J. Yoshinaga, Y. Yanagisawa, M. Endo and J. Takahashi, *Analytical Sciences*, 2003, **19**, 1413-1416.
21. M. Krachler, W. Domej and K. J. Irgolic, *Biological Trace Element Research*, 2000, **75**, 253-263.
22. P.-T. Cheng, K. P. H. Pritzker, M. E. Adams, S. C. Nyburg and S. A. Omar, *Journal of Rheumatology*, 1980, **7**, 609-616.
23. P. T. Cheng and K. P. H. Pritzker, *Journal of Rheumatology*, 1983, **10**, 769-777.
24. D. Gunther, D. Bleiner, M. Guillon, B. Hattendorf and I. Horn, *Chimia*, 2001, **55**, 778-782.
25. B. Hattendorf and D. Gunther, *Journal of Analytical Atomic Spectrometry*, 2000, **15**, 1125-1131.
26. P. R. D. Mason, *Short Course Series - Mineralogical Association of Canada*, 2001, **29**, 63-81.
27. J. Fietzke, A. Eisenhauer, N. Gussone, B. Bock, V. Liebetrau, T. F. Nagler, H. J. Spero, J. Bijma and C. Dullo, *Chemical Geology*, 2004, **206**, 11-20.
28. B. Jackson, S. Harper, L. Smith and J. Flinn, *Analytical and Bioanalytical Chemistry*, 2006, **384**, 951-957.
29. J. Feldmann, A. Kindness and P. Ek, *Journal of Analytical Atomic Spectrometry*, 2002, **17**, 813-818.
30. K. M. D. Jaovisidha and A. K. M. D. Rosenthal, *Current Opinion in Rheumatology*, 2002, **14**, 298-302.
31. C. A. Scotchford and S. Y. Ali, *Osteoarthritis and Cartilage*, 1997, **5**, 107-119.
32. R. Lagier and C. A. Baud, *Pathology, Research and Practice*, 2003, **199**, 329-335.
33. P. B. Halverson, *Current Opinion in Rheumatology*, 1996, **8**, 259-261.
34. P. Z. Vroon, B. Wagt, J. M. Koornneef and G. R. Davies, *Analytical and Bioanalytical Chemistry*, 2008, **390**, 465-476.
35. S. J. Fallon, M. T. McCulloch, R. van Woesik and D. J. Sinclair, *Earth and Planetary Science Letters*, 1999, **172**, 221-238.
36. R. L. Wortmann, H. R. J. Schumacher, M. A. Becker and L. M. Ryan, eds., *Crystal-Induced Arthropathies; Gout, Pseudogout and Apatite-associated Syndromes*, Taylor & Francis, New York, 2006.